Electronic Supplementary Material (ESI) for Physical Chemistry Chemical Physics.

Supporting Information:

Porosity Controls the Catalytic Activity of Platinum Nanoparticles

Wenmiao Yu[a], Christopher Batchelor-McAuley[a], Xin Chang[a], Neil P. Young [b] and Richard G. Compton[*a]

[a] Physical and Theoretical Chemistry Laboratory, Department of Chemistry, University of Oxford, South Parks Road, Oxford OX1 3QZ, United Kingdom

[b] Department of Materials, University of Oxford, Parks Road, Oxford OX1 3PH, United Kingdom

*corresponding author email: Richard.Compton@chem.ox.ac.uk

Contents

Section 1: Transmission Electron Microscopy Characterisation

In this work the structure of the platinum nanoparticle clusters has been extensively investigated and characterized used transmission electron microscopy. Samples were prepared for imaging by depositing 5 µL of a stock PtNP suspension onto a 200 mesh carbon grid coated with holey carbon film (Agar Scientific, Stansted, UK). After dropcasting, grids were left to dry overnight under vacuum before examination. ImageJ software developed at the National Institutes of Health was used to analyse all images. For the atomic resolution microscopy images the citrate was removed from the sample by hydroxide washing the material before it was deposited onto the TEM grid, this was undertaken to minimize carbon build-up during imaging.

1.1 HR-CTEM and nanoparticle size distribution

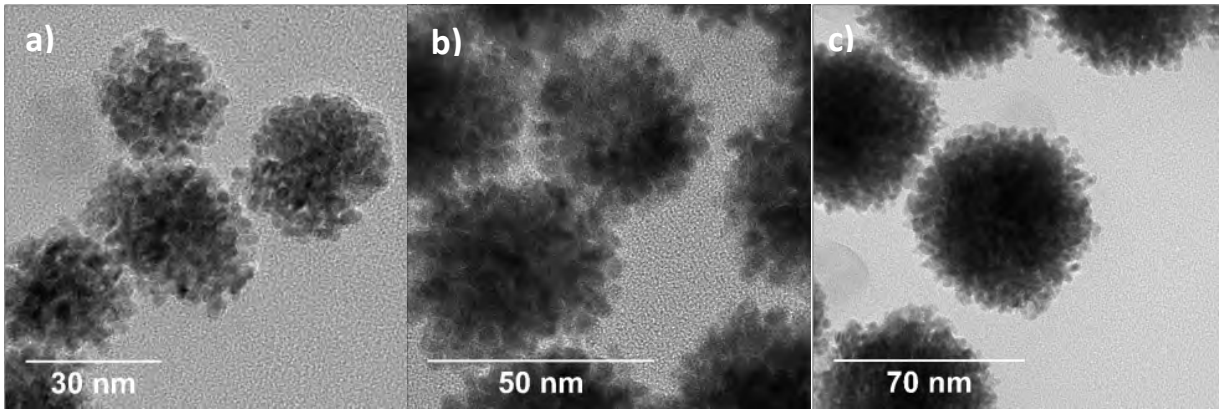

Figure SI 1.1 HR-CTEM images of the mesoporous Pt nanoparticles sample of nominal size a) 30 nm, b) 50 nm and c) 70 nm

High-resolution conventional transmission electron microscopy images were recorded on a JOEL-3000F FEGTEM with an accelerating voltage of 300 kV. These images, examples of which are shown in Figure SI 1.1, were used to evidence the overall particulate structure of the platinum nanoparticles and to provide a measure of their length scale. The nanoparticle size was determined by measuring the 2D projected area of the nanoparticles and converting this measured area into an effective diameter. Figure SI 1.2 plots the measured size distributions for the three nanoparticle samples.

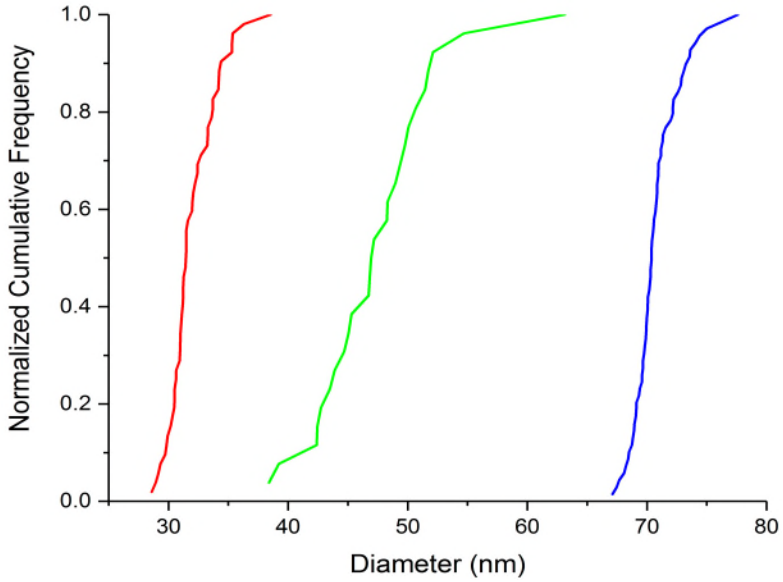

Figure SI 1.2 A plot of normalized cumulative frequency against particle diameter for the Pt nanoparticles of nominal sizes 30 nm (red), 50 nm (green) and 70 nm (blue) with mean diameters measured from 30.6 ± 2.0 nm (n = 47), b) 47.0 ± 3.6 nm (n=50), c) 71.4 ± 2.4 nm (n=74), respectively.

1.2 Electron tomography

The above 2D HR-CTEM images clearly demonstrate that the particles are formed by the aggregation of smaller nanoparticle crystallites. An important question is, 'how porous are these particles'? In order to answer this question conventional transmission electron microscopy tomography was employed. Tomographic imaging of the 30 nm particle sample was undertaken. The dual-axis tilt-series of the platinum nanoparticle aggregates was acquired using a FEI Talos 200c FEG-TEM at a 73000 × magnification, with a pixel size of 1.431 Å per pixel. The dual-axis series consists of two perpendicular tilt-series that are combined for reconstruction. The tilt-series were reconstructed using IMOD 4.9 to give tomograms as a series of z-stacked images. Figure SI 1.3 depicts an example reconstructed z-slice through a number of particles evidencing that the particle are porous throughout their structure.

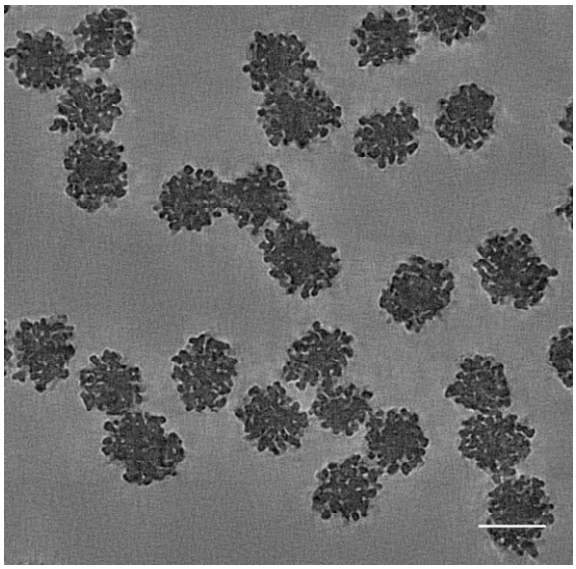

Figure SI 1.3 Tomographic reconstruction of a z-slice through multiple 30 nm platinum nanoparticles evidencing their internal mesoporous structure. Scale bar 30 nm.

1.3 Atomic resolution microscopy

From the HR-TEM images it was observed on close inspection that the platinum nanoparticle structures were highly crystalline and that the substituent particles appeared to be relatively aligned. In order to investigate the extent to which the nanoparticle crystallinity was correlated across the larger aggregate structure and to evidence the presence of defects, aberration corrected high-angle annular dark field scanning transmission electron microscopy was used. These microscope images were acquired on a JEOL ARM-200F with a cold field emission source, Cs corrected probe and 200 kV acceleration voltage.

Here we successfully visualized the particles at the edge of a 50 nm aggregate. Figure SI 1.4 depicts two ARM images of a platinum aggregate nanoparticle at different magnification levels. The crystallinity of the material is clear with individual columns of atoms fully resolved. Figure SI 1.4 b) is the same image as shown in the main manuscript, however in the main text the image has been FFT filtered (and cropped) to minimize some of the image brightness and emphasize the local crystallinity. The same line defect is observable is both images of the particle.

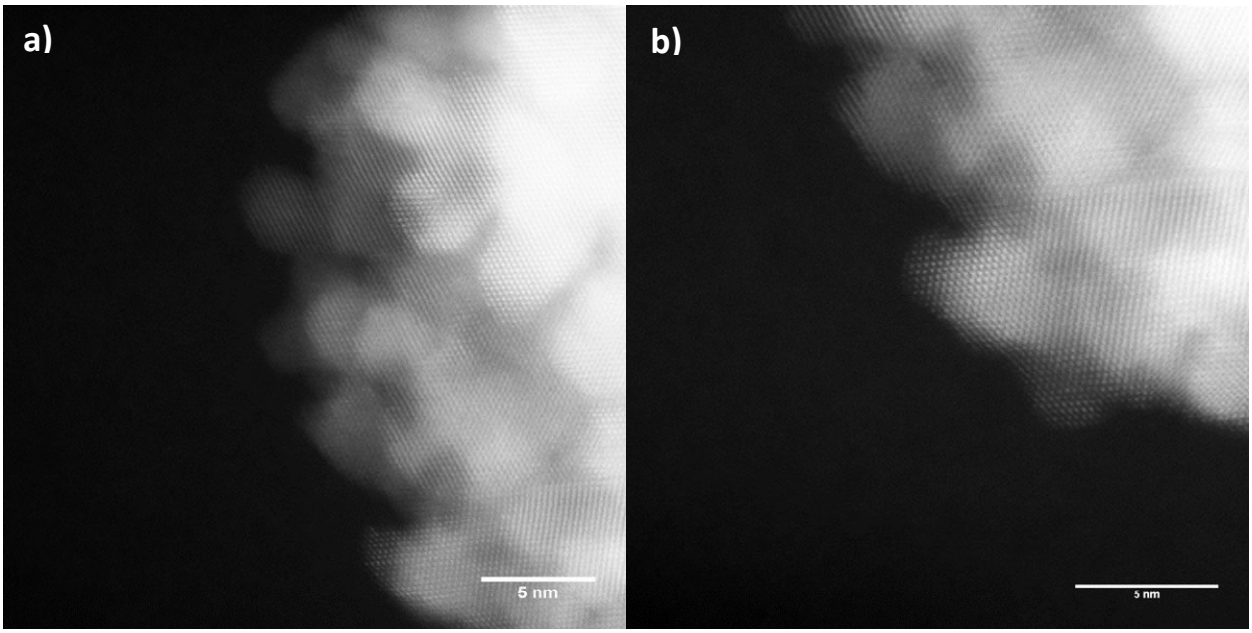

Figure SI 1.4: ARM HAADF-STEM image of the 50 nm platinum nanoparticle sample and two different magnification levels.

Section 2: Hydrogen Oxidation at Platinum Macroelectrode

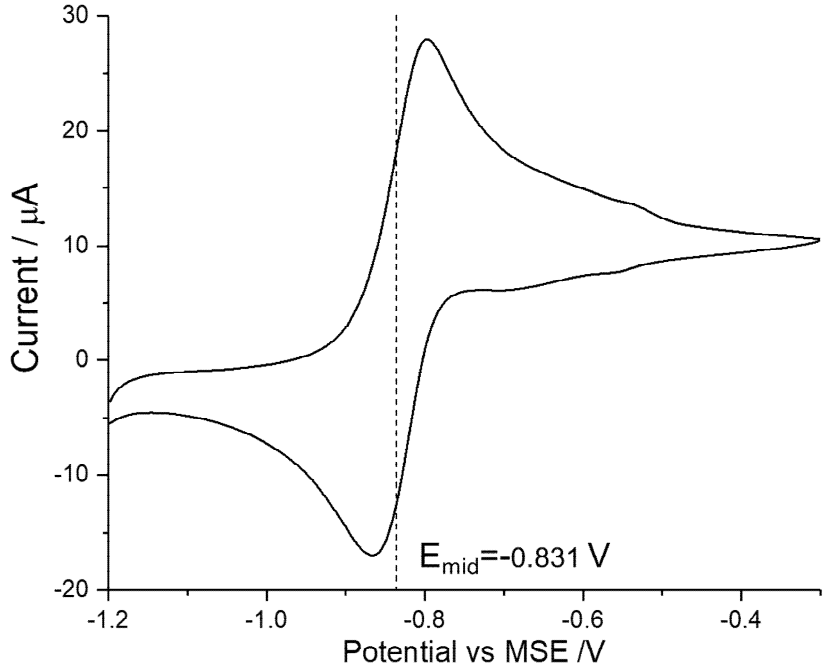

Figure SI 1.1 Voltammetric response of platinum towards the oxidation of hydrogen $[H_2]_{sat}$ = 0.78 mM at Pt macroelectrode (radius = 0.8 mm) at a scan rate of 200 mv s^{-1} in 0.2 M $NaNO_3$, initially scanned anodically from -1.2 V. Showing the reversible oxidation of hydrogen, the reversible half-wave potential (~E_{mid}) as predicted theoretically has been marked on for comparison.

Voltammetrically at the macroscale the oxidation of hydrogen is a reversible processes. Figure SI 2.1 shows the cyclic voltammetric response of a macro polycrystalline platinum electrode in a hydrogen saturated solution.

Section 3: Electrochemical Single Nanoparticle Surface Areas

Single nanoparticle electrochemical measurements are used to give a measure of the surface areas associated with the particle in the three platinum nanoparticle samples. In the presence of hydrogen the measured oxidative spike in current can be used to give a direct measure of the charge transferred per Pt nanoparticle aggregate impact. The theoretical value for the charge transferred per Pt nanoparticle aggregate can be calculated from an estimation of its total surface area (based on a close-packed arrangement of 5 nm Pt spheres to form a spherical Pt nanoparticle aggregate) and the monolayer coverage of H_{upd} on a platinum surface, 2.1 C m^{-2}.[1] There is good agreement between the experimental and theoretical spike areas. However, the accuracy of this theoretically predicted value is predicated on the size of the individual crystallites being prciesely known. In reality a distribution of crystallite sizes are observed, moreover the 30 nm particles exhbit slightly smaller crystallite diameters. The theortical numbers provided here are used simply as a guide and to demonstrate that the measured charges are not inconsitent with the known size and morphology of the particles.

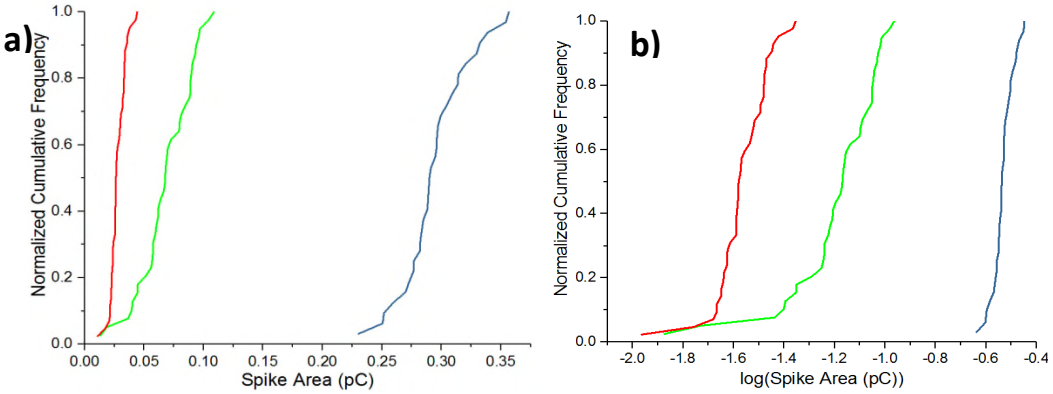

Figure SI 3.1 A plot of the normalized cumulative frequency against the spike area for the Pt nanoparticle aggregates with nominal diameters of 30 nm (red), 50 nm (green) and 70 nm (blue) with mean spike areas calculated to be 0.028 pC (n=42), 0.069 pC (n=39) and 0.295 pC (n=32) respectively.

Pt NP Nominal Diameter (nm)	Theoretical Charge Transfer per Pt NP (pC)	Experimental Spike Area (pC)
30	0.028	0.03 ± 0.006
50	0.10	0.07 ± 0.022
70	0.36	0.30 ± 0.029

Table SI 3.1 Comparing the theoretical charge transfer per Pt nanoparticle aggregate impact and the experimentally measured spike area for the Pt NPs of diameters 30.6 nm, 47.0 nm and 71.4 nm. Deviation from the expected charge transfer increases with aggregate diameter.

Section 4: Hydrogen Peroxide Platinum Catalysed Decomposition

The catalytic decomposition of hydrogen peroxide was studied under alkaline conditions using UV-vis spectroscopy.

4.1 Determination of the concentration of hydrogen peroxide

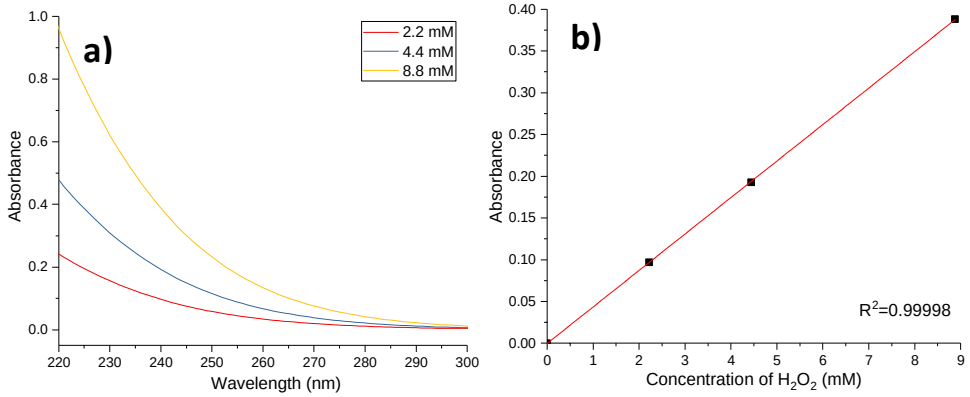

Figure SI 4.1 (a) The absorbance spectra of hydrogen peroxide at various concentrations and (b) calibration for hydrogen peroxide.

In this work, the concentration of hydrogen peroxide in the solution was determined by a spectrophotometric method based on Beer-Lambert law:

$A = \varepsilon LC$

where A is the measured absorbance, ε is the wavelength-dependent molar extinction coefficient (ε_{H2O2} = 43.6 $M^{-1}cm^{-1}$ at 240 nm^{1})[2], L is the pass length and C is the concentration. In order to obtain absorbance in an analytically meaningful range, the stock hydrogen peroxide solution was diluted 1000 to 4000 times with ultrapure water. Figure SI 4.1 shows that hydrogen peroxide exhibits a broad absorbance peak in the UV range, and the measured absorbance at 240 nm of hydrogen peroxide with various concentration were employed to generate the calibration curve (Figure SI 4.1 b). Good correlation coefficients (R^2 = 0.99998) indicated that the 240 nm peak could be used to adequately convert absorbance readings to concentrations.

4.2 Hydrogen peroxide decomposition at PtNPs

In order to study the effect of concentration of PtNPs on the hydrogen peroxide decomposition process, we monitored the absorbance at 240 nm of 1.25 mM H_2O_2 and 20 mM KOH solution initially containing 0.4185 pM, 0.8375 pM and 1.6750 pM 30 nm PtNPs, respectively. The absorbance at 240 nm of all the solutions containing various concentration of PtNPs decreased with the increase of the decomposition

time. The absorbance approached 0.4129, 0.4167 and 0.3863 after 5 min of decomposing, corresponding to ca. 3.0%, 5.4% and 11.3% removal of H_2O_2 from the solution (the absorbance of PtNPs were subtracted during the calculation).

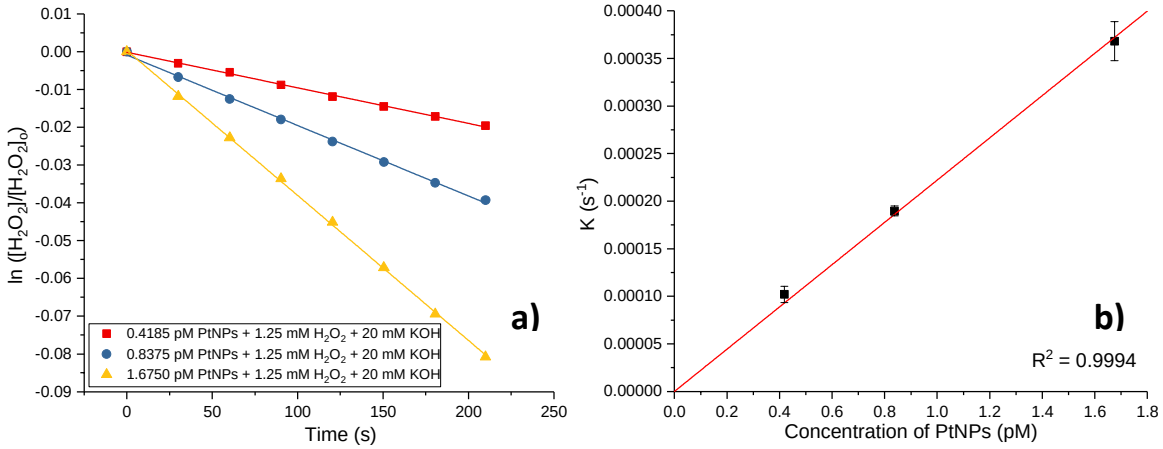

Figure SI 4.2 Hydrogen peroxide platinum nanoparticle catalyzed decomposition, 30 nm PtNPs at 25 °C; (a) Plot of ln([H_2O_2]/[H_2O_2]o) versus time of the hydrogen peroxide decomposition at various concentrations of PtNPs; and (b) the measured pseudo first order rate constants versus the used concentration of PtNPs.

On the basis of the linear regression developed from Figure SI 4.2 and the absorbance at 240 nm, we calculated the concentrations of H_2O_2 during the decomposition process. As shown in Figure SI 4.2 a), the decomposition of H_2O_2 at various concentration of PtNPs were all fitted well based on the first-order kinetics.

The derived rate constants versus concentration of 30 nm PtNPs were plotted in Figure SI 4.2 b), which demonstrated that the Pt catalysed disproportion reaction rate was first order with respect to the PtNPs concentration.

Table SI 4.2 Analysis of PtNPs provided by nanoComposix, San Diego, USA.

Diameter (nm)	Particle Concentration (particles/ml)	Mass Concentration (mg/ml)	Platinum Purity
30	$1.8x10^{11}$	0.053	99.99 %
50	$3.3x10^{10}$	0.051	99.99 %
70	$1.2x10^{10}$	0.052	99.99 %

Section 5: Heterogeneous Catalytic Rate Constants

Using Equation 8 of the main text, the single particle second order rate constants for both the hydrogen oxidation reaction (at -0.5 V vs Ag/AgCl) and the hydrogen peroxide decomposition were re-expressed as a heterogeneous rate constants (m s^{-1}) for the reaction. The magnitude of this heterogeneous rate constant is first, important in providing insight into the catalytic abilities of the nanomaterial and second, is of direct relevance when considering the rate of reaction versus the rate of material mass-transport to and from the catalytic interface. Figure SI 5.1 plots these derived heterogeneous rate constants for the platinum catalyzed oxidation of hydrogen as a function of the measured nanoparticle surface area.

Both reactions are measured to have higher rate constants on the 50 nm particles as compared to the 30 and 70 nm samples.

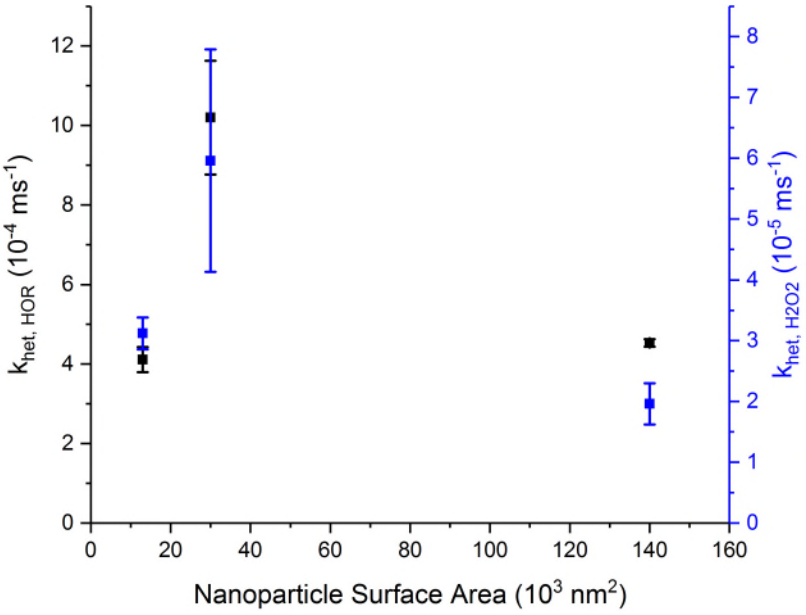

Figure SI 5.1: Derived heterogeneous rate constants for the platinum catalyzed oxidation of hydrogen (at -0.5 V vs Ag/AgCl) and the decomposition of hydrogen peroxide.

Reference

[1] S. Trasatti and O. A. Petrii, *Pure Appl. Chem.*, 1991, **63**, 711-734

[2] A.G. Hildebrandt and I. Roots, *Archives of Biochemistry and Biophysics*, 1975, 171, 385-397.